The Sognefjell volcanic-subvolcanic complex – A late Sveconorwegian arc imbricated in the central Norwegian Caledonides

F. Corfu[1]

Department of Geosciences and CEED, University of Oslo, PB 1047 Blindern, N-0316 Oslo, Norway

ABSTRACT

The Sognefjell volcanic-subvolcanic complex is a composite unit underlying the Jotun Nappe Complex in the southern Norwegian Caledonides. The identity and origin of the complex have been highly debated in past decades, one interpretation considering the rocks to be highly deformed orthogneisses of the Jotun Nappe Complex and the other extreme considering them to be partly of volcanic origin and defining a Caledonian suture. In this study some critical components of the complex have been dated by U-Pb yielding ages of 961 ± 11 Ma for gabbro and 949 ± 4 Ma for a tonalite. A tuffite includes euhedral zircon crystals with ages of 985 to 955 Ma, suggesting derivation from the same magmatic complex. Zircon in an orthogneiss points instead to an older age close to 1600 Ma suggesting that this is a sliver of the Jotun Nappe Complex. A thin straight pegmatite cutting mafic gneiss is 949 ± 3 Ma. Titanite grains in the various rocks range in age from about 970 to 890 Ma, demonstrating that the dominant metamorphism was Sveconorwegian with minimal resetting in spite of the likely Caledonian deformation. The new observations, combined with published data, support the notion that these rocks are of volcanic-subvolcanic origin, but show that they are late Sveconorwegian, not Caledonian as originally envisaged. They likely developed in an arc complex at the margin of Baltica and possibly within the realm of the Asgard Sea. Arc magmatism was coeval with lower crustal processes in parts of the Baltic craton that would eventually become Caledonian nappes.

1. Introduction

In the literature the Grenville, Sveconorwegian and Sunsaas orogens, in Laurentia, Baltica and Amazonia, respectively, are often considered to have been connected at 1000–900 Ma, but details of geometry and timing of convergence and later divergence remain largely speculative and debated. In traditional paleogeographical models the Sveconorwegian Orogen is placed along the eastward projection of the Grenville Orogen, a link supported by the parallel age zonation, from Archean to Neoproterozoic, of the respective hinterlands. In detail, however, the composition and chronology of the two orogens are considerably different so that the real plate configurations remain uncertain (e.g. Slagstad et al., 2018, 2019). The Amazonian craton is inferred to have collided with Laurentia at 1100–1000 Ma, but its relation to Baltica is unconstrained and open to diverse speculations. An important element playing a role in these reconstructions is an assemblage of clastic sedimentary rocks produced in the late stages of formation of these orogens and now dispersed in Caledonian allochthons on both sides of the Atlantic and in the Arctic (e.g. Kirkland et al., 2007). Cawood et al. (2010) postulated deposition of these sediments in an

oceanic basin, the Asgard Sea, opened by the rifting and clockwise rotation of Baltica from Laurentia sometime before 990 Ma. These sedimentary rocks were then deformed, metamorphosed and locally intruded by a suite of granites (Renlandian suite) between 980 and 920 Ma (e.g. Johansson et al., 2000; Kirkland et al., 2006; Corfu et al., 2007; Cutts et al., 2009; Bird et al., 2018). Subsequent stages of tectonomagmatic activity followed in what Cawood et al. (2010) call the Valhalla exterior accretionary Orogen.

In the Scandinavian Caledonides elements linked to the Asgard Sea occur in association with nappes in part derived from Baltica and in part of more exotic origin, often in complex arrangements that obscure their origins and the timing and processes of their juxtaposition. A potential element of this system also occurs in the region around the Jotun Nappe Complex (JNC) in southern Norway (Figs. 1, 2). On its northwestern side, between Lom and Sogndal, the JNC is underlain by an imbricate assemblage of sedimentary, volcanic and plutonic rocks, structurally arranged in a mostly inconsistent manner. One of the components in this assemblage is an extensional mélange interpreted to have formed in the initial stages of the Caledonian cycle (Andersen et al., 2012; Jakob et al., 2017). The origin and age of other elements in
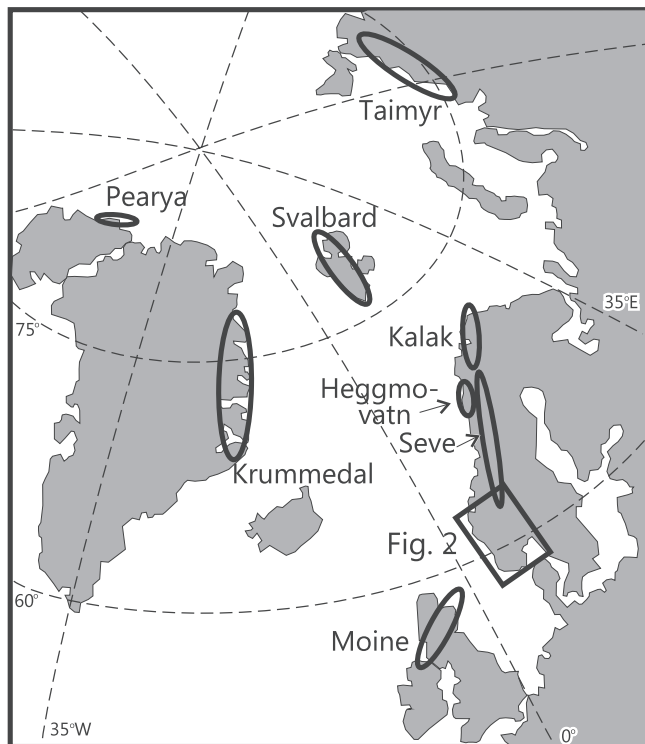
Fig. 1. Location of the area of study and regions mentioned in the text.

this sub-JNC stack remain poorly understood. These include the Sognefjell volcanic-subvolcanic complex (SVSC), the object of the present investigation (Figs. 2 and 3). The SVSC comprises rocks of clear sedimentary origin, rocks of clear magmatic origin, and others that are of uncertain derivation, either metamorphosed and deformed supracrustal rocks or deformed orthogneisses. Their origin has been the subject of controversy and speculations, especially their deformation history and implications for the question of the provenance of the JNC and location of a potential suture (see below). The paper reports new observations and U-Pb ages for this unit, clearing up previous misunderstandings and establishing a basis for reconsidering their place in the Sveconorwegian – Valhalla realm and the events affecting Baltica and surrounding basins in the final stages of the Sveconorwegian Orogeny.

2. Geological setting

2.1. The Lom-Sogndal imbricate stack

The geological complexity of the area, with large lithological variations both across and along strike, has led to several different classifications and definitions of geological units. From northwest to southeast (Fig. 3) the dominant features are: (1) the crystalline basement of the Western Gneiss Complex, composed largely of Precambrian orthogneiss and granite; (2) the top of the basement – a generally sheared interface inclined at about 20–30° to the east; (3) a cover of phyllite and schist, mostly parautochthonous to allochthonous; (4) meta-arkose; (5) variably sheared orthogneisses; and on top (6) high grade gneisses of the Upper Jotun Nappe. Whereas the bottom (Western Gneiss Complex) and top (Upper Jotun Nappe) are coherent units exhibiting lateral continuity, the intervening units are very discontinuous and the presence or absence, relative position and thickness of units 3–5 can vary substantially. In the 1:250,000 Årdal map of Lutro and Tveten (1996) the, mostly tectonically low, sequence of schists and phyllites (no. 3) is assigned to the Fortun-Vang Nappe (cf. Milnes and Koestler, 1985). These rocks are Cambro-Ordovician, as indicated by fossils further east in south Norway and also by detrital zircons in this region (Slama and

Pedersen, 2015). In parts of Bøverdalen this unit includes prominent solitary serpentinites, which together with various schists, marbles, conglomerates and orthogneiss slivers have been interpreted to represent hyperextension mélange, a unit that can be followed discontinuously to the Bergen area (Jakob et al., 2017). Meta-arkose (no. 4) tends to occur mainly close to orthogneisses of the Lower Jotun Nappe, but in detail its distribution can be very variable. These rocks were named the Turtagrø Zone by Milnes and Koestler (1985) and are considered an equivalent of the Late Precambrian Valdres Group (sparagmite), an arkose with characteristic purple feldspar, widespread to the east of the JNC.

### 2.2. Sognefjell volcanic subvolcanic complex

The rocks forming the SVSC, the focus of this paper, are interpreted as mixtures of arkose and sheared orthogneiss (nos. 4 and 5) in the compilation map of Lutro (2002), whereas Tilston (1983) distinguished several more specific units. The map shown in Fig. 3 is based primarily on the compilation of Lutro (2002) but integrates elements of the interpretation of Tilston (1983). The sequence above the Western Gneiss Region consists of moderately southeast-dipping quartzites, various schists, arkoses, mafic rocks, rocks of apparent volcanic origin, and orthogneisses, in part similar to, and in part distinct from those present in the JNC (Banham, 1968; Banham et al., 1979; Tilston, 1983). The top of the sequence is occupied by crystalline rocks of the JNC, itself separated into a lower unit of amphibolite facies, mostly highly deformed rocks (Lower Jotun Nappe), and an upper unit of granulite-facies rocks (Upper Jotun Nappe). The base of the JNC has been defined in several ways, either to include only the crystalline rocks proper (e.g. Tilston, 1983), or also a zone of mixed crystalline slices and meta-arkoses (e.g. Lutro, 2002).

2.3. Evolution of concepts

Banham et al. (1979) interpreted the rocks of the SVSC, or more precisely their sequence of Sygnefjell sparagmite, Turtagrø metavolcanics and Helgedalen metagreywackes, to represent a Paleozoic assemblage formed in a subduction setting. They also interpreted the structural evidence as indicating thrusting of the JNC to the northwest, implying that it represented an up-thrusted segment of the lower crust derived from the Faltungsgraben, and combined these features to postulate the occurrence of a 'Jotunheim Caledonian Suture', expanding a notion formulated much earlier by Goldschmidt (1912). The concept of a suture below the JNC has also been discussed by Andersen and Andresen (1994) based on the occurrence of 'ophiolitic' rocks and serpentinites underneath the JNC and related nappes. More recent work (Andersen et al., 2012; Jakob et al., 2017) demonstrates that the serpentinite lenses and related lithologies are part of a tectonic mélange formed through hyperextension of continental crust and the exhumation and local denudation of upper mantle peridotites, but the mélange is not part of the SVSC.

The interpretation of a northwest-directed thrusting of the nappe, proposed by Banham et al. (1979), was disputed by Roberts (1977) and Milnes and Koestler (1985), both showing that the evidence of northwest kinematics referred to a set of late structures related to extension whereas the earlier structures and other evidence supported the notion of a far travelled allochthon arriving from the northwest (e.g. Hossack et al., 1985). This interpretation has been further substantiated by detailed structural analyses on the regional scale (e.g. Andersen, 1998; Fossen, 2010) and in the JNC (e.g. Lundmark and Corfu, 2008b).

Meanwhile the nature and significance of the 'Turtagrø metavolcanics' has remained uncertain, some concluding that the rocks were highly sheared orthogneisses (Bryhni et al., 1981; Lutro, 2002), rather than metavolcanic rock as suggested by Banham et al. (1979). Tilston (1983) re-examined and described the geology of the Sognefjell area in detail. Immediately above the crystalline basement of the Western
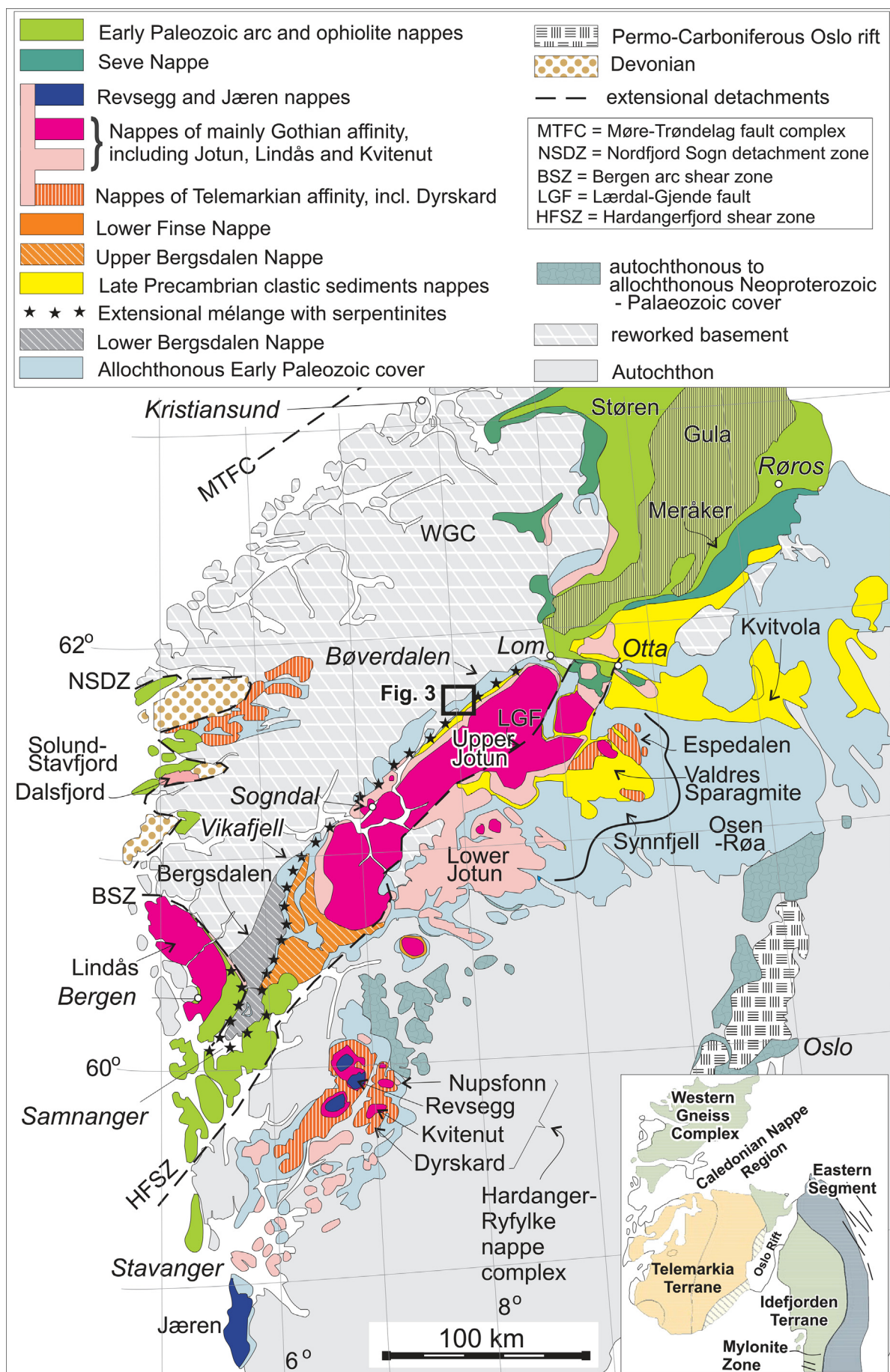
Fig. 2. Simplified tectonic map of southern Norway displaying the units discussed in the text and the location of Fig. 3 (modified from Corfu et al., 2014).
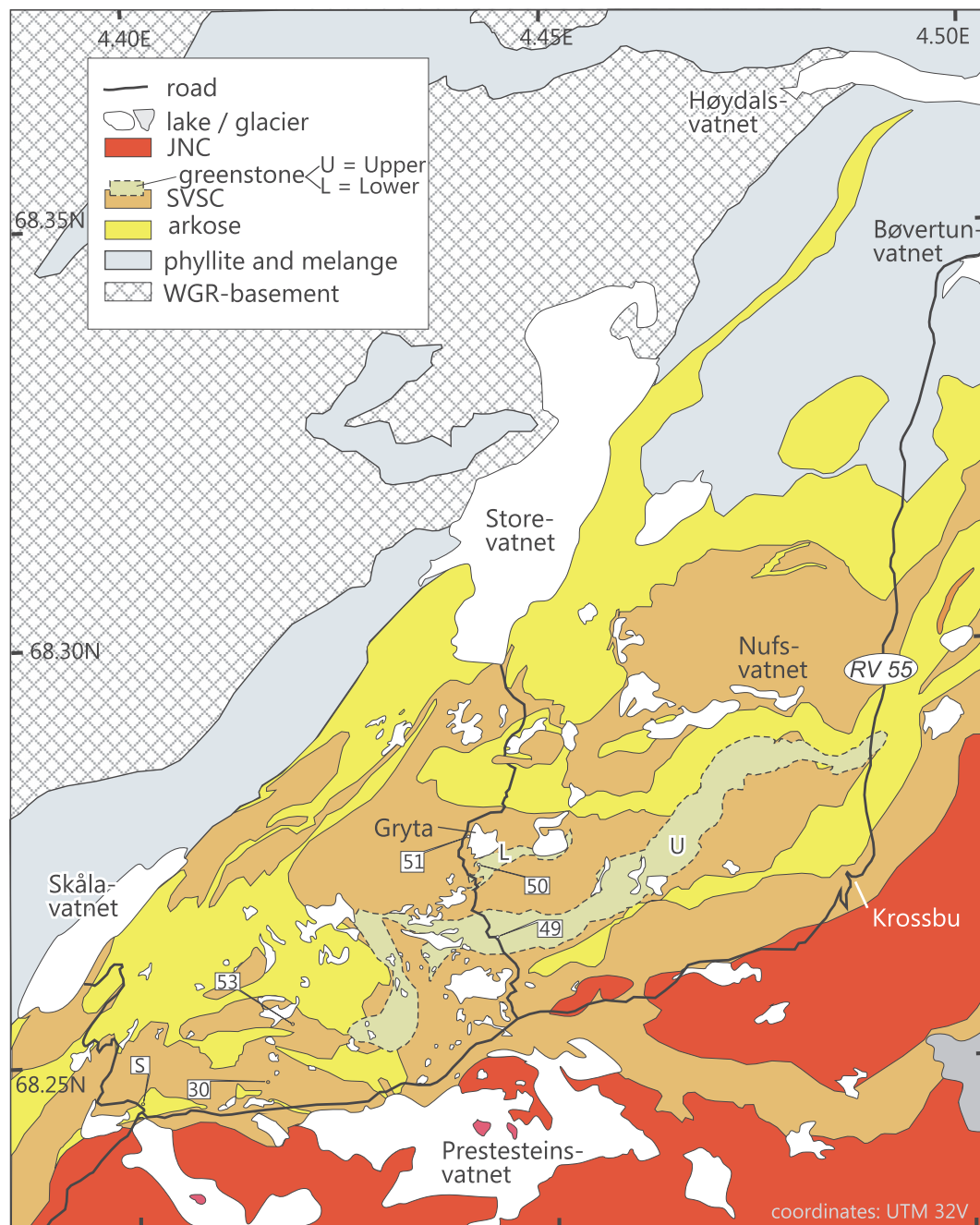

Fig. 3. Simplified geological map of the Sognefjell area based on Lutro (2002), partially modified according to Tilston (1983) and own observations.

Gneiss Region in the north he distinguished a lower unit of schists and quartzites with a mostly sheared contact, but locally with a basal conglomerate. He interpreted the unit as parautochthonous, likely corresponding to the Fortun Formation of Milnes and Koestler (1985). This is overlain by a mixed assemblages which includes (i) a synclinally folded succession of calcareous rocks (Bovertun meta-limestones) (ii) a conglomeratic unit dominated by quartzite pebbles (Vassenden conglomerate), (iii) meta-arkoses (Sygnefjell meta-arkose), and (iv) the Sygnefjell greenstones (Fig. 3).

2.4. The Sygnefjell greenstones

Tilston (1983) distinguished two greenstone layers. The principal rock type in these units is described as a massive, fine grained, dark green rock, in part with a diffuse banding defined by variations from mafic to more leucocratic bands. There is a gradual increase upwards of meta-arkosic and schistose units. Major element analyses reported by Tilston (1983) indicate a calc-alkaline affinity of the lower greenstones and tholeiitic affinity of the upper greenstones while Ti, Zr and Nb abundances suggest an intraplate origin as continental tholeiites. The REE patterns are fractionated with moderate enrichments in LREE ($La_N = 50–100$ and $Lu_N = 10–20$) and weak positive Eu anomalies. Tantalum and Nb display negative anomalies.

2.5. Orthogneisses

Gneiss units of likely magmatic origin are common, especially in the middle and upper parts of the assemblage. Tilston (1983) designated several different occurrences, for example the monzogabbroic (or monzodioritic) Dyrhaugan Gneiss spatially associated with the lower greenstone. The gneiss is locally cut by mafic dykes and pegmatites. Other orthogneiss units are present through the area. Most of these orthogneisses are felsic, but mafic gneisses are also observed. They are in various stages of deformation, but locally retain magmatic textures.

3. U-Pb geochronology

3.1. Samples

Five samples were investigated in this study. Sample 50 (C-07-50) represents a mylonitic felsic augen gneiss outcropping close to Lake Gryta (Fig. 3) in the area of the lower greenstone of Tilston (1983). The rock is highly mylonitic with sparse plagioclase porphyroclasts, local aggregates of recrystallized quartz, and little fine-grained biotite and sericite.

Sample 51 (C-07-51) is from a set of outcrops in the same area on the shore of Lake Gryta. It is a sheared tonalite to diorite characterized by stretched aggregates of hornblende and antiperthitic plagioclase and sparse sericite in a strongly mylonitic matrix. The unit is cut by mafic dykes, but locally the two phases appear to be co-mingling (Fig. 4A). Gabbroic rocks are common in this area and represent the 'Dyrhaugan Gneiss' unit of Tilston (1983).

Metagabbro sample 53 (C-07-53) was collected further west from a boudin, a few meters wide, which floats within a succession of variegated highly deformed gneisses (Fig. 4B–C). The sample is medium grained and has escaped the deformation affecting the margins of the boudin, but the primary minerals are highly retrogressed, with very fine grained chlorite, sericite and opaques surrounding clusters of hornblende.

The fourth sample 30 (C-16-30) represents a banded rock (Fig. 4D) characterized by the presence of discrete quartz and feldspar crystals in a grey, fine-grained matrix. The rock is considered a tuffaceous deposits. In thin section it is dominated by a recrystallized fine grained matrix with larger clasts of perthitic microcline and plagioclase together with titanite, and little biotite and sericite.

Sample 49 is one of several thin and straight pegmatite veins cutting massive mafic gneiss (Fig. 4F) in Tilston's (1983) Upper Greenstone Belt.

3.2. Analytical procedure

Geochronology was carried out by ID-TIMS U-Pb following the basic procedure developed by Krogh (1973). The most fundamental modifications are the use of a mixed ^{202}Pb-^{205}Pb-^{235}U spike, the much lower blank and sample sizes, the more advanced mass spectrometry and data reduction procedures, and the single stage HBr-HCl chemical separation used for titanite analyses. More details of the procedure for this lab are given in Corfu (2004). Zircon was subjected to air abrasion (Krogh, 1982) or chemical abrasion (Mattinson, 2005). Decay constants are from Jaffey et al. (1971). The data were corrected for blanks of ≤2 pg Pb and 0.1 pg U. Initial common Pb, if present, was corrected using compositions estimated from the Stacey and Kramers (1975) model for the age of the rock, except for titanite in sample 49, which was corrected with the Pb composition of coexisting feldspar. Data were plotted and calculated using the program Isoplot (Ludwig, 2009). All uncertainties are given at the 2s level.

3.3. Results

For augen gneiss sample 50 four zircon grains were analyzed

(Table 1). The first two analyses were done on zircon tips treated with air abrasion. Two subsequent analyses were of a tip and a prism that were chemically abraded. The four analyses are discordant and slightly scattered (Fig. 5). The two analyses on chemically abraded grains lie on a line projecting to 1632 Ma and with a lower intercept age of 837 Ma. The two other analyses plot below the line indicating the effects of younger Pb loss.

The tuffitic rock (sample 30) contains a large zircon population, dominated by heterogeneous subrounded grains, which are likely of xenocrystic origin. Euhedral zircon crystals are also present and a selection of such grains was analyzed. Five grains yield concordant to slightly discordant data points with ages between 980 and 957 Ma. Titanite is also common in this sample and the analyzed grains yield ages of about 970 Ma, 950, 935, 895 and 865 Ma. The last two were from pale coloured, low U and low Th/U grains, the type that often forms by secondary processes.

The gabbro (53) yielded few zircon fragments, pinkish and with inclusions. Three analyses were obtained from air abraded grains. Another batch of grains was chemically abraded, but only one grain survived that treatment. Three of the analyses are about 2–3% discordant, and together with a fourth, 14% discordant analysis define a line with an upper intercept age of 961 ± 11 Ma and a Caledonian lower intercept age.

The tonalitic gneiss (51) contains a population of equant to short-prismatic zircon grains, mostly variously subrounded and low in U. Three analyses of zircon treated with air abrasion are essentially concordant, but one is imprecise due to a high level of common Pb. Projecting the data from a Caledonian lower intercept age yields an upper intercept age of 949 ± 4 Ma. Titanite occurs as brown, mostly somewhat turbid fragments. Two analyses, one of air abraded grains, are imprecise due to high initial Pb contents of 8–10 ppm (for 40–80 ppm U). The titanite analyses plot below the zircon data. Their position could be due either to partial resetting because of Caledonian Pb loss or to a late Sveconorwegian overprint, in which case the concordia age of 899 ± 11 Ma would be relevant.

Zircon from the pegmatite (49) consists of euhedral short prismatic grains. The analyses show some scatter reflecting the presence of small amounts of inherited Pb, most evident in the oldest data point (992 Ma, Table 1). The other analyses are more tightly grouped, the three youngest defing an intercept of 949 ± 3 Ma (Fig. 5). Three analyses of titanite indicate low U and relatively high initial Pb contents yielding imprecise data with $^{206}Pb/^{238}U$ ages between 932 and 902 Ma. The grains have granular surfaces suggesting superficial reworking or overgrowths and the fact that abrasion reduced the discordance suggests that the spread was caused by partial resetting during the Caledonian events.

4. Discussion

4.1. Chronology of the late Sveconorwegian complex

The most fundamental change in our understanding of the SVSC with respect to previous assumptions (e.g. Banham et al., 1979) is the recognition that it cannot be correlated with Paleozoic supracrustal rocks but its origin must be considered in a Sveconorwegian tectonic framework.

Zircons for the gabbro yield an age of 961 ± 11 Ma, older than the tonalite which is dated at 949 ± 4 Ma. The tonalite is itself intruded by, and intermingles with gabbroic rocks (Fig. 4A). Thus, magmatism appears to have been a more protracted event of 10 m.y. or more. The appearance and composition of the surrounding supracrustal rocks suggests that intrusive and supracrustal rocks were all part of a common volcanic-subvolcanic complex. This is supported by the ages of 980–957 Ma for the zircons analyzed in the tuffitic rock, as the sharp euhedral nature of the grains is consistent with a local derivation. The rest of the zircon population in the tuffitic rock shows distinct rounding

Fig. 4. A: Tonalite intermingling with gabbro inclusion (at lake Gryta); B: gabbro lens in variegated gneisses (sample location of 53); C: Detail of B – strong lithological variation of the gneiss envelope; D: banded tuffite, location of sample 30; E: finely laminated and folded gneiss – typical occurrence in the SVSC; F: mafic gneiss with prominent lineation cut by thin pegmatite vein (near hammer; sample 49).

and heterogeneity, and could in part be older than 980 Ma. The oldest dated titanite grains in the tuffitic rock have ages of 950 and 945 Ma, but it is not clear whether they are also detrital or whether they formed during metamorphism.

Slama (2016) studied detrital zircons in a sample of arkose collected not very far from the site of the tuffitic rock (site S in Fig. 3) yielding ages between about 1750 and 900 Ma, whereby the youngest ones cannot be distinguished from 950 Ma within their errors. A similar range may be expected also for the bulk zircon population in the tuffitic rock. Interestingly, about 15% of the grains in the population analyzed by Slama (2016) yield ages between about 980 and 950 Ma, suggesting

a local derivation of these grains from the SVSC. As the author does not provide information on the morphology of the grains it is not possible to establish a closer comparison. The arkose has been assumed to be a member of the Ediacaran Valdres Sparagmite (Lutro and Tveten, 1996) but because of the absence of post 950–900 Ma detrital grains the alternative that the arkose may be a Late Sveconorwegian deposit could be considered.

4.2. Pre-Sveconorwegian components

The augen gneiss zircons indicate an older age than gabbro and

Table 1
U-Pb data, Sognefjell.

Characteristics[1]	Weight [μg][2]	U [ppm][2]	Th/U[3]	Pbi[4] [ppm]	Pbc[5] [pg]	206Pb/204Pb[6]	207Pb/235U[7]	2σ	206Pb/238U[7] [abs]	2σ	rho	207Pb/206Pb[7]	2σ	206Pb/238U[7] [Ma]	2σ	207Pb/235U[7] [Ma]	2σ	207Pb/206Pb[7] [Ma]	2σ	D[8] [%]
50 – augen gneiss, Lake Gryta, 61°34.534/7°56.812 (C-07-50)																				
Z eu-sb tip AA [1]	1	263	0.67	0.00	0.8	4969	3.410	0.013	0.25241	0.00085	0.93	0.09799	0.00014	1450.9	4.3	1506.8	3.0	1586.3	2.6	9.5
Z eu-sp CA [1]	6	103	0.69	0.00	1.1	8493	3.281	0.008	0.24901	0.00052	0.93	0.095549	0.000086	1433.4	2.7	1476.5	1.9	1538.9	1.7	7.6
Z eu-sb tip AA [1]	1	352	0.44	0.00	1.1	4465	2.885	0.011	0.22515	0.00081	0.94	0.09293	0.00012	1309.0	4.3	1378.0	3.0	1486.5	2.5	13.2
Z eu-sp CA [1]	1	323	0.46	0.00	1.3	3188	2.4502	0.0075	0.20320	0.00047	0.85	0.08745	0.00014	1192.5	2.5	1257.5	2.2	1370.5	3.1	14.2
51 – foliated tonalite, Lake Gryta, 61°34.719/7°56.730 (C-07-51)																				
Z eu-sb sp AA [3]	19	25	1.06	3.71	75	80	1.554	0.055	0.15956	0.00089	0.04	0.0706	0.0025	954.3	5.2	951.9	22.0	946	72	-0.9
Z eu-sb sp AA [11]	35	31	0.84	0.10	5.7	1891	1.546	0.005	0.15857	0.00035	0.82	0.07072	0.00012	948.8	1.9	949.0	1.9	949.3	3.6	0.1
Z eu-sb sp AA [18]	29	30	0.93	0.13	5.9	1459	1.536	0.005	0.15771	0.00034	0.78	0.07064	0.00014	944.0	1.9	944.9	1.9	947.0	4.0	0.3
T fr NA [1]	11	46	4.53	10.18	114	59	1.413	0.080	0.14804	0.00139	0.07	0.0692	0.0039	890.0	7.9	894.3	33.3	905	113	1.8
T fr br NA [1]	11	79	3.26	8.05	14	71	1.418	0.053	0.15038	0.00091	0.20	0.0684	0.0025	903.1	5.3	896.7	22.3	881	74	-2.7
53 – gabbro, 61°33.274/7°53.934 (C-07-53)																				
Z an fr CA [1]	1	77	0.76	0.00	0.6	1308	1.524	0.007	0.15631	0.00044	0.70	0.07073	0.00024	936.2	2.5	940.2	2.8	950	7	1.5
Z an fr AA [2]	1	88	0.93	0.00	1.4	637	1.526	0.014	0.15562	0.00048	0.55	0.07111	0.00058	932.4	2.7	940.8	5.8	961	17	3.1
Z an fr AA [1]	1	151	0.95	4.99	7.1	223	1.507	0.019	0.15518	0.00065	0.44	0.07044	0.00082	930.0	3.7	933.3	7.8	941	24	1.3
Z an fr br AA [1]	1	253	1.12	0.27	2.3	824	1.0644	0.0079	0.11614	0.00035	0.59	0.06647	0.00041	708.3	2.0	736.0	3.9	821	13	14.5
30 – tuffite, 61°34.6/7°53'50.9 (C-16-30)																				
Z eu sp CA [1]	9	97	0.25	0.00	0.9	9560	1.626	0.005	0.16418	0.00036	0.87	0.07182	0.00010	979.9	2.0	980.2	1.8	980.8	2.8	0.1
Z eu tip CA [1]	5	219	2.71	0.00	1.9	5818	1.593	0.005	0.16156	0.00035	0.80	0.07151	0.00013	965.4	1.9	967.4	1.9	971.9	3.6	0.7
Z eu sp CA [1]	9	195	0.85	0.00	2.6	6748	1.579	0.004	0.16059	0.00034	0.91	0.071321	0.000080	960.0	1.9	962.0	1.6	966.6	2.3	0.7
Z eu sp CA [1]	10	116	0.80	0.00	1.4	8016	1.568	0.004	0.15946	0.00033	0.80	0.07134	0.00012	953.8	1.8	957.8	1.8	967.1	3.5	1.5
Z eu tip CA [1]	1	706	0.52	0.00	0.6	12,281	1.574	0.005	0.16084	0.00043	0.90	0.07099	0.00010	961.5	2.4	960.2	2.0	957.3	2.9	-0.5
T an cl NA [1]	15	52	0.05	3.77	62	143	1.596	0.028	0.16266	0.00056	0.15	0.0711	0.0012	971.5	3.2	968.5	11.0	962	35	-1.1
T an br NA [1]	8	100	4.30	4.30	40	208	1.536	0.019	0.15603	0.00046	0.29	0.07138	0.00084	934.7	2.6	944.8	7.6	968	24	3.7
T an br NA [9]	22	150	1.92	4.79	111	305	1.525	0.021	0.15883	0.00081	0.52	0.06965	0.00082	950.3	4.6	940.6	8.3	918	24	-3.8
T an pb NA [3]	11	11	0.11	2.67	35	49	1.423	0.092	0.14907	0.00143	0.03	0.0692	0.0045	895.7	8.3	898.7	38.0	906	128	1.2
T an cl NA [1]	9	14	0.10	4.93	50	40	1.330	0.128	0.14332	0.00198	0.01	0.0673	0.0065	863.4	11.6	858.8	54.8	847	190	-2.1
49 – pegmatite, 61°34.026/7°57.106 (C-07-49)																				
Z eu tip + sp CA [2]	1	191	0.77	0.00	5.7	343	1.585	0.025	0.15911	0.00045	0.38	0.0722	0.0011	951.8	2.5	964.2	9.7	993	30	4.4
Z eu tip CA [1]	24	38	0.72	0.00	4.2	2156	1.5519	0.0053	0.15822	0.00034	0.71	0.07114	0.00017	946.9	1.9	951.2	2.1	961.4	4.9	1.6
Z eu tip CA [1]	31	44	0.99	0.00	3.0	4491	1.5547	0.0043	0.15866	0.00034	0.86	0.07107	0.00010	949.3	1.9	952.4	1.7	959.4	3.0	1.1
Z eu sp CA [1]	29	31	1.14	0.00	1.4	6096	1.5523	0.0042	0.15853	0.00035	0.89	0.071018	0.000089	948.6	1.9	951.4	1.7	957.9	2.6	1.0
Z eu tip CA [1]	12	29	1.11	0.00	1.1	3180	1.5543	0.0046	0.15918	0.00034	0.81	0.07082	0.00012	952.2	1.9	952.2	1.8	952.2	3.6	0.0
Z eu tip CA [1]	7	45	0.80	0.00	1.1	2768	1.5509	0.0050	0.15906	0.00037	0.80	0.07072	0.00014	951.5	2.1	950.9	2.0	949.3	3.9	-0.3
Z eu sp CA [1]	5	88	0.98	0.00	0.7	6209	1.5429	0.0040	0.15835	0.00033	0.87	0.070670	0.000092	947.6	1.8	947.7	1.6	947.9	2.7	0.0
T an br AA [1]	2	58	5.27	6.35	19	76	1.526	0.026	0.15546	0.00051	0.33	0.0712	0.0012	931.5	2.8	941.0	10.4	963	33	3.6
T an br NA [1]	10	9	7.73	2.05	27	48	1.526	0.046	0.15283	0.00063	0.32	0.0724	0.0021	916.8	3.5	941.0	18.4	998	58	8.7
T an br NA [8]	75	15	7.67	6.23	478	38	1.526	0.064	0.15012	0.00057	0.44	0.0737	0.0030	901.7	3.2	940.8	25.5	1034	80	13.7

1) Z = zircon; T = titanite; eu = euhedral; sb = subhedral; an = anhedral; sp = short prismatic (l/w = 2–4); fr = fragment; pb = pale-brown; br = brown; [1] = number of grains in fraction; NA = non abraded, AA = air abraded; CA = chemically abraded; unless otherwise specified all the zircons were clear and transparent.

2) Weight and concentrations are known to better than 10%, except for those near and below the ca. 1 μg limit of resolution of the balance.

3) Th/U model ratio inferred from 208/206 ratio and age of sample.

4) Pbi = initial common Pb (less blank).

5) Pbc = total common Pb in sample (initial + blank).

6) Raw data corrected for fractionation and blank.

7) Corrected for fractionation, spike, blank and initial common Pb; error calculated by propagating the main sources of uncertainty. Initial common Pb correction based on the model of Stacey and Kramers (1975), except for titanite in sample 49 which was corrected with Pb from co-existing feldspar: 206/204 = 16.538 ± 0.041 and 207/204 = 15.359 ± 0.050.

8) D = degree of discordancy.
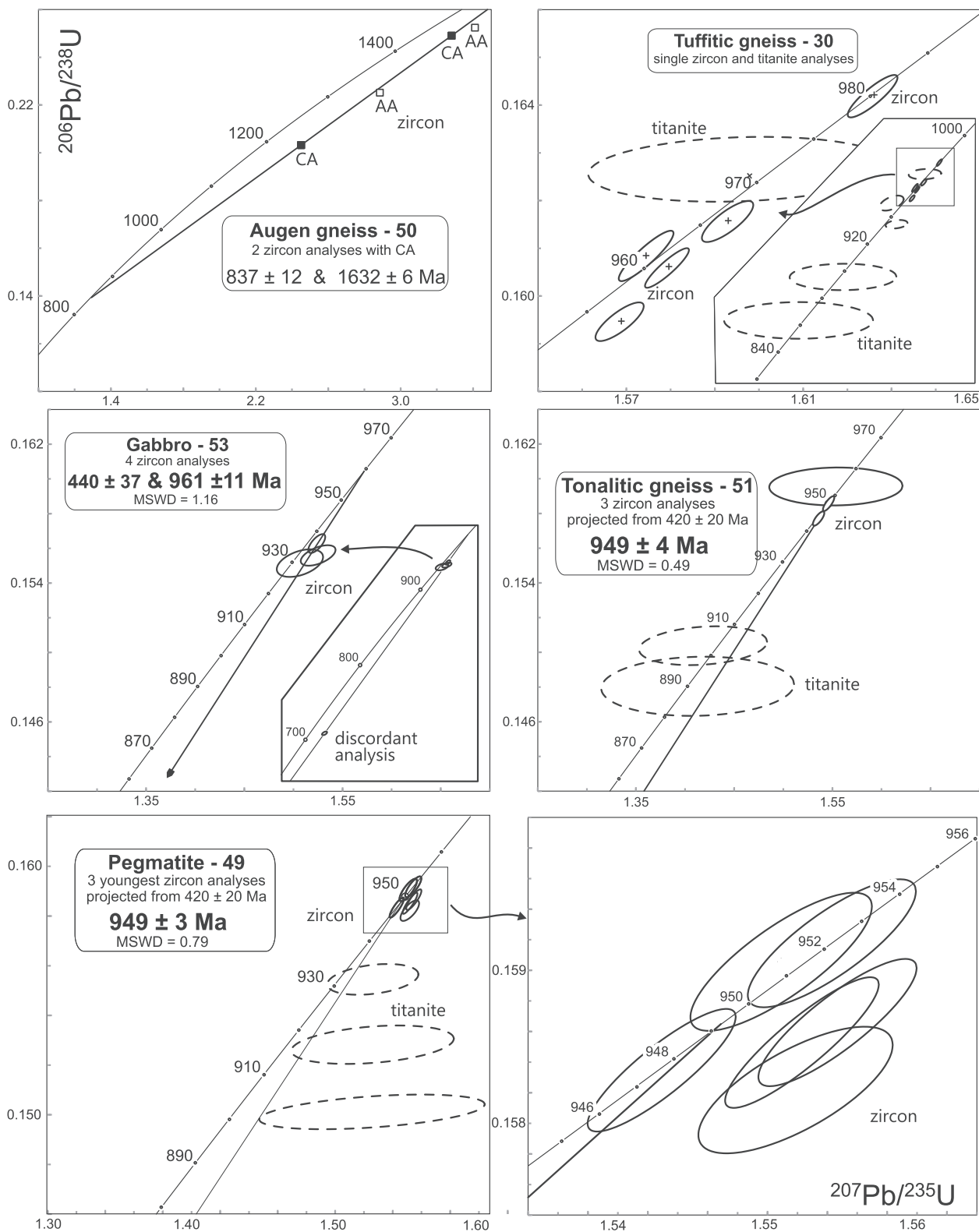
Fig. 5. Concordia diagrams with data for rocks of the Sognefjell volcanic-subvolcanic complex. Ellipses indicate 2 sigma uncertainty for zircon (full lines) and titanite (dashed lines) analyses.

tonalite, and also a very different type of discordance pattern. The scatter of the four zircon analyses prevents an exact determination but the two analyses of chemically abraded grains alone point to an upper intercept age of 1632 Ma, which is in the age range of the main mass of the gneisses in the JNC (Lundmark et al., 2007). A typical feature of zircon data in the Jotun gneisses is also the distinct discordance along

lines having lower intercept ages of 950–900 Ma (e.g. Schärer, 1980), the latter corresponding to the time of new zircon growth in leucosomes (Lundmark et al., 2007). In the augen gneiss the lower intercept age is somewhat lower at 837 Ma, but this is likely an effect of the Caledonian overprint which tilted the line. The effect of secondary Pb loss is seen more strongly in the two grains only treated with air abrasion, and is

also evident in zircon of the gabbro and the tonalite. The similarity of the augen gneiss U-Pb pattern and age to the gneisses in the JNC suggests incorporation of slices of JNC gneiss into the imbricate stack.

4.3. Rocks of uncertain affinity

Within the SVSC Tilston (1983) outlined several gneiss units which he considered to be part of a potential basement to the volcanic-subvolcanic complex. One of the orthogneisses on his map, however, appears to coincide with the location of the sampled tonalite (949 Ma) suggesting that some of the orthogneisses are the product of Sveconorwegian magmatism rather than a pre-existing basement (the tonalite sample was collected from outcrops in a perennial snow field, and the level of exposure may have changed over the years).

Mafic gneiss of the Upper Greenstone has a well developed foliation and lineation which are cut by straight, unstrained pegmatites (sample 49), the age of which sets a lower limit of 949 Ma for the time of this deformation. The age of the pegmatite coincides with that of the tonalite, which, however, is hosted by the highly deformed low-grade supracrustal rocks and is itself variably deformed. It is thus possible that, although coeval, the tonalite and the pegmatite may not be genetically and spatially related. One possibility is that mafic gneiss of the Upper Greenstone represents slices of the JNC. The alternative is that it represents a basement unit of the SVSC that remained screened from the later deformation affecting most supracrustal and intrusive rocks.

4.4. Origin of the Sognefjell volcanic-subvolcanic complex

In the original interpretation of Banham et al. (1979) the SVSC was envisaged as the product of an island arc-trench system. Based on geochemical information Tilston (1983) concluded that the mafic rocks were most compatible with an origin as continental tholeiites. The structures suggestive of magma mingling and contemporaneous intrusion of mafic and felsic magma (Fig. 4A) would be consistent with such a process, perhaps in a back arc setting.

There are no obvious analogues of the SVSC in the region. The closest candidates could be in the Bergsdalen Nappe Complex (Fig. 2), which has a very similar tectonic position as the SVSC, sandwiched between the Western Gneiss Region and the Jotun and Lindås nappe complexes, and interleaved with sheets of phyllite, mica-schists and melange (e.g. Fossen, 1993; Jakob et al., 2017). The Bergsdalen Nappe Complex is composed largely of supracrustal rocks including mafic and felsic volcanic rocks and clastic sediments together with gabbros and granites (Fossen, 1993), but their ages are not well known. Fossen (1993) lists a number of Rb-Sr whole rock ages ranging from about 1300 to 950 Ma for various volcanic and granitic rocks, but there are no modern U-Pb data available yet.

The SVSC was formed during the same orogenic period that caused high grade metamorphism, deformation and magmatism in the JNC. Between 980 and 900 Ma the rocks of the JNC were in the lower crust undergoing high-grade metamorphism, local anatexis and extensive deformation (Lundmark et al., 2007). And at around 965 Ma a part of the nappe complex was intruded by the large Inner Sogn anorthosite complex (Lundmark and Corfu, 2008a). By contrast, the SVSC was never exposed to high grade metamorphic conditions and thus must have evolved at shallow crustal levels, as indicated by the association of gabbro and tonalite with a variety of rocks of apparent volcanic origin and related metasedimentary rocks, and the low metamorphic grade recorded by their mineral assemblages. There is also not much affinity between the magmatic lithologies in the two settings, AMCG rocks in the JNC and tonalite-gabbro and related volcanics in the SVSC. These distinctions do not support a direct connection between the SVSC and the JNC and it appears more likely that they evolved in distinct settings and only became aggregated later, either in the late stages of the Sveconorwegian orogeny, or, more likely, during the Scandian collision.

4.5. The Sognefjell volcanic-subvolcanic complex in a Sveconorwegian context

Modern interpretations of the Svecorwegian orogeny place the event in an active margin setting with subduction and the construction of an extensive magmatic arc between 1060 and 1030 Ma, followed by shallowing of the subducting slab producing compression in parts of the orogen and the high pressure rocks at the Idefjorden Terrane boundary (see inset in Fig. 2). In this interpretation the late orogenic magmatism between 980 and 930 Ma is taken to reflect extension in a back arc setting during rapid slab rollback and retreat of the trench (Slagstad et al., 2013, Slagstad et al., 2017, 2018).

While large parts of the present Sveconorwegian autochthon record extensive magmatism and metamorphism between 1060 and 1020 Ma (e.g. Bingen et al., 2008; Coint et al., 2015; Bingen and Viola, 2018) there is so far no evidence for magmatic or metamorphic activity between 1060 and 1000 Ma in the JNC. Thus, before 1000 Ma the JNC and related nappes were probably located outside of the zones affected by arc magmatism and associated events. In the Hardanger-Ryfylke Nappe Complex (Fig. 2) a compressional event at 1000 Ma juxtaposed and welded the Kvitenut Nappe, which comprises Gothian elements similar to the JNC, on the Dyrskard Nappe of Telemarkian affinity (Roffeis et al., 2013). This episode heralded the intense lower crustal processes with magmatism, metamorphism and deformation between 980 and 900 Ma recorded in all Gothian nappes (Roffeis and Corfu, 2014). At that stage the Jotun and Lindås nappe complexes would have been parts of continental crust several hundred kilometers further northwest of their present position and in the post 990 Ma orogenic period underwent widespread deformation, metamorphism at amphibolite to granulite facies conditions, and local AMCG magmatism.

An active margin model can thus account both for the mid- to lower crustal development of the rocks in JNC and the contemporaneous development of the SVSC further outboard in an arc or back arc position. The complex deformation and late Sveconorwegian metamorphism indicated by the youngest titanites in the SVSC may support a juxtaposition of the two systems already in the final stages of the Sveconorwegian orogeny, by extension and uplift of the JNC onto the SVSC. But at present this hypothesis lacks direct evidence.

4.6. Potential connection to the Valhalla orogen

The Grenvillian and Sveconorwegian orogens have conventionally been considered to have formed by plate interactions between Laurentia, Baltica and Amazonia and the intervening Mirovoi Ocean (e.g. Cawood and Pisarevsky, 2017). The Grenvillian Orogeny between 1080 and 980 Ma (Gower and Krogh, 2002; Hynes and Rivers, 2010) was the concluding episode of long-lasting subduction and accretionary processes at the southern margin of Laurentia culminating with the collision of Laurentia with a continent, presumably Amazonia (e.g. Carr et al., 2000). Magmatism had ceased by about 980 Ma across most of the orogen, with exception of its edge in southeastern Labrador where intrusions of discrete granitic, alkalic and anorthositic dykes and plutons are recorded between 980 and 955 Ma (Gower and Krogh, 2002; Heaman et al., 2004).

By contrast, the Sveconorwegian Orogen was affected by bimodal magmatism throughout much of the period between 980 and 930 Ma, culminating at around 930 Ma with the intrusion of widespread granitic plutons and the Rogaland anorthosite complex (e.g. Schärer et al., 1996; Vander Auwera et al., 2003; Andersen et al., 2007; Slagstad et al., 2018). There are thus fundamental differences between the two orogens and the traditionally assumed link is tenuous, as argued by Slagstad et al. (2019). The arc related rocks of the SVSC described in this paper provide further support for the presence of a subduction system at the margin of the Sveconorwegian orogen. Such a subduction system cannot fit, spatially and temporally, into most of the traditional models that link Grenville and Sveconorwegian orogens in a triple junction
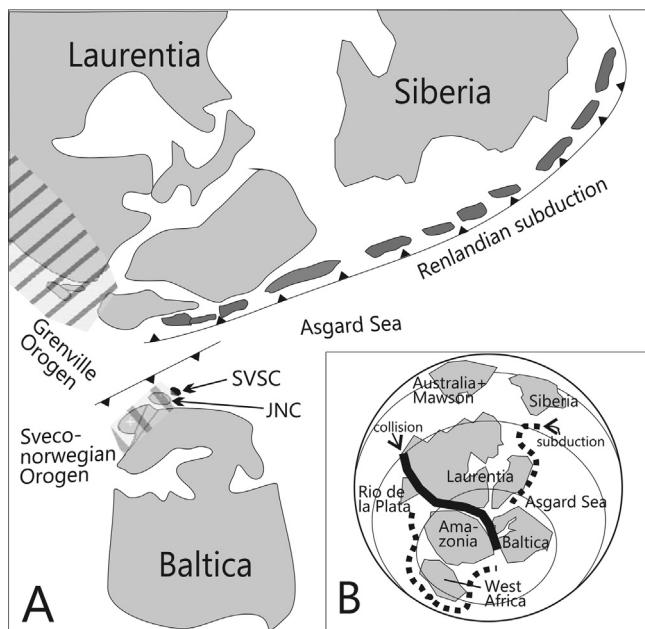
Fig. 6. A: Conceptual paleogeographic setting of the Sveconorwegian Orogen and potential links to the Neoproterozoic accretionary Valhalla Orogen. The relative positions of Laurentia and Baltica are constrained by the paleomagnetically defined latitudes, in this representation approximately vertical. There are no firm constraints for the longitudes, except for geological considerations, and thus the position of Baltica relative to Laurentia is undefined. The position of Siberia with respect to Laurentia follows crudely Pisarevsky et al. (2008).The 'Renlandian subduction' system proposed by Cawood et al. (2010) is here linked to the analogous system in Taimyr along northern Siberia, following Priyatkina et al. (2017). The subduction system responsible for formation of the SVSC, and also for magmatic and metamorphic processes in the crust at the margin of Baltica, including the Jotun Nappe Complex (JNC), can be envisaged as having been an element within the Asgard Sea, analogous to the ensemble of tectonic events concurrently active in the modern Western Pacific region. B: Traditional concept on the aggregation of continents at southern latitudes at about 990 Ma, here according to Cawood and Pisarevsky (2017). The closeness of Baltica, Laurentia and Amazonia is a common feature in many reconstructions but, while the latitudes are based on paleomagnetic arguments, their longitudinal positions are dictated only by geological considerations. It is evident that such a configuration leaves no space for the development of the SVSC.

with the proposed collisional partner Amazonia (Fig. 6B) (e.g. Bogdanova et al., 2008; Ibanez-Mejia et al., 2011).

Cawood et al. (2010) suggested that, after rifting from Laurentia at around 1270 Ma, by 990 Ma Baltica had undergone a 90° clockwise rotation, opening the Asgard Sea. The latter became the site of deposition of thick syn- and post- orogenic detritus derived from the Grenville and Sveconorwegian mountains. Between about 980 and 920 Ma these clastic sedimentary rocks were metamorphosed and deformed and locally intruded by a suite of granites (Renlandian granites) and in places volcanic rocks. None of these rocks occur in autochthonous positions but they are all dispersed in allochthonous terranes in Scotland (Moine), East Greenland (Krummedal), Norway (Kalak, Seve, Heggmovatn), and throughout the Arctic on Svalbard, the Pearya terrane in Ellesmere Island and in central Taimyr (Fig. 1) (e.g., Johansson et al., 2000; Albrecht, 2000; Pease et al. 2001; Watt and Thrane, 2001; Kirkland et al., 2006; Corfu et al., 2007; Cutts et al., 2009; Strachan et al. 2010; Vernikovsky et al. 2011; Agyei-Dwarko et al. 2012; Augland et al., 2014; Gasser, 2014; Malone et al. 2017; Priyatkina et al. 2017; Bird et al., 2018). Cawood and Pisarevsky (2017) suggest that the granites are arc related, as indicated by their geochemistry, and developed over a subduction system, which they place along the margin of Laurentia. For Taimyr, Vernikovsky et al. (2011)

postulate an arc system peripheral to Siberia. Because of the allochthonous nature of all these terranes the reconstructions remain conjectural. Fig. 6A combines elements from Cawood et al. (2010) and Priyatkina et al. (2017) and serves to illustrate the general concept of a system of related arc in the Asgard Sea that initiated the Valhalla Orogen. Common elements of all these terranes are the presence of ca. 1 Ga clastic sedimentary rocks, evidence of metamorphism and/or magmatism between 980 and 940 Ma, in part with one or more subsequent Neoproterozoic clastic sequences, and in part affected by tectonometamorphic events at 870–800 Ma, at around 700 Ma and/or around 600 Ma.

The SVSC tends to be compositionally different than the dominant type of rocks in the Valhalla Orogen, being less evolved and richer in mafic components. Because of the coevality with the initial events of the Valhalla Orogen, and the apparent spatial connections, the two systems may have been related, as suggested in Fig. 6A. A combination of active arcs, basins and collisional orogens resembling the tectonism in the present day Western Pacific – Himalaya region could explain the relationships between these different units. Thus, the possibility remains that, rather than being Sveconorwegian, the SVSC was actually an exotic elements derived from the Valhalla orogen.

5. Summary

The SVSC is a tectonic assemblage with fragments of ca. 1600–1700 Ma continental crust, clastic sediments and volcanic-subvolcanic rocks formed in late Sveconorwegian time. It includes 961 ± 11 Ma gabbro and 949 ± 4 Ma tonalite. Euhedral zircons in a tuffite yield a range of ages between 985 and 955 Ma. A thin straight pegmatite cutting a mafic gneiss also yields an age of 949 ± 3 Ma showing that parts of the complex where already deformed at the time of intrusion of the latest phases. The new data and observations demonstrate that this complex is not Paleozoic, as originally thought, but likely an arc or back-arc formed in the latest stages of the Sveconorwegian orogeny at the margin of Baltica and the Asgard Sea. The coevality with the lower crustal processes that formed the JNC could be the result of distant effects of a common subduction system.

Acknowledgements

References

Agyei-Dwarko, N.Y., Augland, L.E., Andresen, A., 2012. The Heggmovatn supracrustals, North Norway – a late Mesoproterozoic sequence of Laurentian origin in the Scandinavian Caledonides? Precamb. Res. 212–213, 245–262.

Albrecht, L.G., 2000. Early structural and metamorphic evolution of the Scandinavian Caledonides: A study of the eclogite-bearing Seve Nappe Complex at the Arctic Circle, Sweden. PhD thesis. Lund University.

Andersen, T., Griffin, W.L., Sylvester, A.G., 2007. Sveconorwegian underplating in southwestern Fennoscandia: LAM–ICPMS U-Pb and Lu–Hf isotope evidence from granites and gneisses in Telemark, southern Norway. Lithos 93, 273–287.

Andersen, T.B., Andresen, A., 1994. Stratigraphy, tectonostratigraphy and the accretion of outboard terranes in the Caledonides of Sunnhordland, W. Norway. Tectonophysics 231, 71–84.

Andersen, T.B., 1998. Extensional tectonics in the Caledonides of southern Norway, an overview. Tectonophysics 285, 333–351.

Andersen, T.B., Corfu, F., Labrousse, L., Osmundsen, P.-T., 2012. Evidence for hyperextension along the pre-Caledonian margin of Baltica. J. Geol. Soc., London 169, 601–612. https://doi.org/10.1144/0016-76492012-011.

Augland, L.E., Andresen, A., Corfu, F., Agyei-Dwarko, N.Y., Larionov, A., 2014. The Bratten-Landegode gneiss complex: a fragment of Laurentian continental crust in the Uppermost Allochthon of the Scandinavian Caledonides. In: Corfu, F., Gasser, D., Chew, D.M. (Eds.), New Perspectives on the Caledonides of Scandinavia and Related Areas. Geological Society, London, pp. 633–654 doi: 10.1144/SP390.1, Special Publications 390.

Banham, P.H., 1968. The basal gneisses and basement contact of the Hestbrepiggan area, north Jotunheimen, Norway. Nor. Geol. Unders. 252, 1–77.

Banham, P.H., Gibbs, A.D., Hopper, F.W.M., 1979. Geological evidence in favour of a Jotunheimen Caledonian suture. Nature 277, 289–291.

Bingen, B., Nordgulen, Ø., Viola, G., 2008. A four-phase model for the Sveconorwegian orogeny, SW Scandinavia. Nor. Geol. Tidsskr. 88, 43–72.

Bingen, B., Viola, G., 2018. The early-Sveconorwegian orogeny in southern Norway: Tectonic model involving delamination of the sub-continental lithospheric mantle. Precambr. Res. 313, 170–204.

Bird, A., Cutts, K., Strachan, R., Thirlwall, M.F., Hand, M., 2018. First evidence of Renlandian (c. 950–940 Ma) orogeny in mainland Scotland: Implications for the status of the Moine Supergroup and circum-North Atlantic correlations. Precambr. Res. 305, 283–294. https://doi.org/10.1016/j.precamres.2017.12.019.

Bogdanova, S.V., Bingen, B., Gorbatschev, R., Kheraskova, T.N., Kozlov, V.I., Puchkov, V.N., Volozh, Y.A., 2008. The East European Craton (Baltica) before and during the assembly of Rodinia. Precambr. Res. 160, 23–45.

Bryhni, I., Bockelie, J.F., Nystuen, J.-P., 1981. The southern Norwegian Caledonides: Oslo-Sognefjord-Ålesund (Excursion A1). Excursion Guide. Uppsala Caledonide Symposium 1981, 151 pp.

Carr, S.D., Easton, R.M., Jamieson, R.A., Culshaw, N.G., 2000. Geologic transect across the Grenville orogen of Ontario and New York. Can. J. Earth Sci. 37, 193–216. https://doi.org/10.1139/cjes-37-2-3-193.

Cawood, P.A., Strachan, R., Cutts, K., Kinny, P.D., Hand, M., Pisarevsky, S., 2010. Neoproterozoic orogeny along the margin of Rodinia: Valhalla orogen, North Atlantic. Geology 38, 99–102.

Cawood, P.A., Pisarevsky, S.A., 2017. Laurentia-Baltica-Amazonia relations during Rodinia assembly. Precambr. Res. 292, 386–397. https://doi.org/10.1016/j.precamres.2017.01.031.

Coint, N., Slagstad, T., Roberts, N.M.W., Marker, M., Røhr, T., Sørensen, B.E., 2015. The Late Mesoproterozoic Sirdal Magmatic Belt, SW Norway: relationships between magmatism and metamorphism and implications for Sveconorwegian orogenesis. Precambr. Res. 265, 57–77. https://doi.org/10.1016/j.precamres.2015.05.002.

Corfu, F., 2004. U-Pb age, setting, and tectonic significance of the anorthosite-mangerite charnockite-granite-suite, Lofoten-Vesterålen, Norway. J. Petrol. 45, 1799–1819. https://doi.org/10.1093/petrology/egh034.

Corfu, F., Roberts, R.J., Torsvik, T.H., Ashwal, L.D., Ramsay, D.M., 2007. Perigondwanan elements in the Caledonian nappes of Finnmark, northern Norway: implications for the paleogeographic framework of the Scandinavian Caledonides. Am. J. Sci. 307, 434–458.

Corfu, F., Andersen, T.B., Gasser, D., 2014. The Scandinavian Caledonides: main features, conceptual advances, and critical questions. In: Corfu, F., Gasser, D., Chew, D.M. (Eds.), New Perspectives on the Caledonides of Scandinavia and Related Areas. Geological Society, London, pp. 9–43 doi: 10.1144/SP390.25, Special Publications 390.

Cutts, K.A., Hand, M., Kelsey, D.E., Wade, B., Strachan, R.A., Clark, C., Netting, A., 2009. Evidence for 930 Ma metamorphism in the Shetland Islands, Scottish Caledonides: implications for Neoproterozoic tectonics in the the Laurentia-Baltica sector of Rodinia. J. Geol. Soc., London 166, 1033–1048. https://doi.org/10.1144/0016-76492009-006.

Fossen, H., 1993. Structural evolution of the Bergsdalen Nappes, southwest Norway. Norges Geol. Undersøkelse Bull. 42, 23–49.

Fossen, H., 2010. Extensional tectonics in the North Atlantic Caledonides: a regional view. In: Law, R.D., Butler, R.W.H., Holdsworth, R.E., Krabbendam, M., Strachan, R.A. (Eds.), Continental Tectonics and Mountain Building: The Legacy of Peach and Horne. Geological Society, London, pp. 767–793 doi: 10.1144/SP335.31, Special Publications 335.

Gasser, D., 2014. The Caledonides of Greenland, Svalbard and other Arctic areas: status of research and open questions. In: Corfu, F., Gasser, D., Chew, D.M. (Eds.), New Perspectives on the Caledonides of Scandinavia and Related Areas. Geological Society, London, pp. 93–129 doi: 10.1144/SP390.17, Special Publications 390.

Goldschmidt, V.M., 1912. Geologisch-Petrographische Studien im Hochgebirge des südlichen Norwegenes. II. Die kaledonische Deformation der südnorwegischen Urgebirgstafel. Videnskapsselskapets Skrifter, I. Mat-naturv. Klasse 19, 11 pp.

Gower, C.F., Krogh, T.E., 2002. U-Pb geochronological review of the Proterozoic history of the eastern Grenville Province. Can. J. Earth Sci. 39, 795–829.

Heaman, L.M., Gower, C.F., Perreault, S., 2004. The timing of Proterozoic magmatism in the Pinware terrane of southeast Labrador, easternmost Quebec and northwest Newfoundland. Can. J. Earth Sci. 41, 127–150. https://doi.org/10.1139/e03-088.

Hossack, J.R., Garton, M.R., Nickelsen, R.P., 1985. The geological section from the foreland up to the Jotun thrust sheet in the Valdres area, south Norway. In: Gee, D.G., Sturt, B.A. (Eds.), The Caledonide Orogen—Scandinavia and Related Areas. Wiley, Chichester, pp. 443–456.

Hynes, A., Rivers, T., 2010. Protracted continental collision – evidence from the Grenville Orogen. Can. J. Earth Sci. 47, 591–620.

Ibanez-Mejia, M., Ruiz, J., Valencia, V.A., Cardona, A., Gehrels, G.E., Mora, A.R., 2011. The Putumayo Orogen of Amazonia and its implications for Rodinia reconstructions: new U-Pb geochronological insights into the Proterozoic tectonic evolution of northwestern South America. Precambr. Res. 191, 58–77. https://doi.org/10.1016/j.precamres.2011.09.005.

Jaffey, A.H., Flynn, K.F., Glendenin, L.E., Bentley, W.C., Essling, A.M., 1971. Precision measurement of half–lives and specific activities of ^{235}U and ^{238}U. Phys. Rev., Section C, Nucl. Phys. 4, 1889–1906.

Jakob, J., Alsaif, M., Corfu, F., Andersen, T.B., 2017. Age and origin of thin discontinuous gneiss sheets in the distal domain of the magma-poor hyperextended pre-Caledonian margin of Baltica, southern Norway. J. Geol. Soc., London 174, 557–571. https://doi.org/10.1144/jgs2016-049.

Johansson, A., Larionov, A.N., Tebenkov, A.M., Gee, D.G., Whitehouse, M.J., Vestin, J., 2000. Grenvillian magmatism of western and central Nordaustlandet, northeastern

Svalbard. Trans. R. Soc. Edinburgh: Earth Sci. 90, 221–254.

Kirkland, C.L., Daly, J.S., Whitehouse, M.J., 2006. Granitic magmatism of Grenvillian and late Neoproterozoic age in Finnmark, Arctic Norway—constraining pre-Scandian deformation in the Kalak Nappe Complex. Precambr. Res. 145, 24–52.

Kirkland, C.L., Daly, J.S., Whitehouse, M.J., 2007. Provenance and terrane evolution of the Kalak Nappe Complex, Norwegian Caledonides: implications for Neoproterozoic palaeogeography and tectonics. J. Geol. 115, 21–41.

Krogh, T.E., 1973. A low-contamination method for hydrothermal decomposition of zircon and extraction of U and Pb for isotopic age determinations. Geochim. Cosmochim. Acta 37, 485–494. https://doi.org/10.1016/0016-7037(73), 90213-5.

Krogh, T.E., 1982. Improved accuracy of U-Pb zircon ages by the creation of more concordant systems using an air abrasion technique. Geochim. Cosmochim. Acta 46, 637–649.

Ludwig, K.R., 2009. Isoplot 4.1. A Geochronological Toolkit for Microsoft Excel. Berkeley Geochronology Center Special Publication, pp. 76 4.

Lundmark, A.M., Corfu, F., Spürgin, S., Selbekk, R.S., 2007. Proterozoic evolution and provenance of the high-grade Jotun Nappe Complex, SW Norway: U-Pb geochronology. Precambr. Res. 159, 133–154. https://doi.org/10.1016/j.precamres.2006.12.015.

Lundmark, A.M., Corfu, F., 2008a. Late-orogenic Sveconorwegian massif anorthosite in the Jotun Nappe Complex, SW Norway, and causes of repeated AMCG magmatism along the Baltoscandian margin. Contrib. Miner. Petrol. 155, 147–163. https://doi.org/10.1007/s00410-007-0233-5.

Lundmark, A.M., Corfu, F., 2008b. Emplacement of a Silurian granitic dyke swarm during nappe translation in the Scandinavian Caledonides. J. Struct. Geol. 30, 918–928. https://doi.org/10.1016/j.jsg.2008.03.008.

Lutro, O.J., Tveten, E., 1996. Geologisk kart over Norge, berggrunnskart Årdal, 1:250000. Geological Survey of Norway.

Lutro, O.J., 2002. Berggrunnskart Sygnefjell 1518 III, M 1:50000, preliminary edition, 1:50000. Geological Survey of Norway, Trondheim.

Malone, S.J., McClelland, W.C., von Gosen, W., Piepjohn, K., 2017. The earliest Neoproterozoic magmatic record of the Pearya terrane, Canadian high Arctic: implications for Caledonian terrane reconstructions. Precambr. Res. 292, 323–349. https://doi.org/10.1016/j.precamres.2017.01.006.

Mattinson, J.M., 2005. Zircon U-Pb chemical abrasion ('CA-TIMS') method: combined annealing and multi-step partial dissolution analysis for improved precision and accuracy of zircon ages. Chem. Geol. 220, 47–66.

Milnes, A.G., Koestler, A.G., 1985. Geological structure of Jotunheimen, southern Norway (Sognefjell – Valdres cross section). In: Gee, D.G., Sturt, B.A. (Eds.), The Caledonide Orogen: Scandinavia and Related Areas. John Wiley and Sons Ltd, pp. 457–474.

Pease, V., Gee, D., Vernikovsky, V., Vernikovskaya, A., Kireev, S., 2001. Geochronological evidence for late-Grenvillian magmatic and metamorphic events in central Taimyr, northern Siberia. Terra Nova 13, 270–280.

Pisarevsky, S., Natapov, L.M., Donskaya, T.V., Gladkochub, D.P., Vernikovsky, V.A., Pisarevsky, S., Natapov, L.M., Donskaya, T.V., Gladkochub, D.P., Vernikovsky, V.A., 2008. Proterozoic Siberia: a promontory of Rodinia. Precambr. Res. 160, 66–76.

Priyatkina, N., Collins, W.J., Khudoley, A., Zastrozhnov, D., Ershova, V., Chamberlain, K., Shatsillo, A., Proskurnin, V., 2017. The Proterozoic evolution of northern Siberian Craton margin: a comparison of U-Pb–Hf signatures from sedimentary units of the Taimyr orogenic belt and the Siberian platform. Int. Geol. Rev. 59, 1632–1656. https://doi.org/10.1080/00206814.2017.1289341.

Roberts, J.L., 1977. Allochthonous origin of the Jotunheim Massif in southern Norway: a reconnaissance study along its northwestern margin. J. Geol. Soc., London 134, 351–362.

Roffeis, C., Corfu, F., Gabrielsen, R.H., 2013. A Sveconorwegian terrane boundary in the Caledonian Hardanger-Ryfylke Nappe Complex: the lost link between Telemarkia and the Western Gneiss Region? Precambr. Res. 228, 20–35. https://doi.org/10.1016/j.precamres.2013.01.008.

Roffeis, C., Corfu, F., 2014. Caledonian nappes of southern Norway and their correlation with Sveconorwegian basement domains. In: Corfu, F., Gasser, D., Che, D.M. (Eds.), New Perspectives on the Caledonides of Scandinavia and Related Areas. Geological Society, London, pp. 193–221 doi:10.1144/SP390.13, Special Publications 390.

Schärer, U., 1980. U-Pb and Rb–Sr dating of a polymetamorphic nappe terrain; the Caledonian Jotun Nappe, southern Norway. Earth Planet. Sci. Lett. 49, 205–218.

Schärer, U., Wilmart, E., Duchesne, J.-C., 1996. The short duration and anorogenic character of anorthosite magmatism: U-Pb dating of the Rogaland complex, Norway. Earth Planet. Sci. Lett. 139, 335–350.

Slagstad, T., Roberts, N.M.W., Marker, M., Røhr, T.S., Schiellerup, H., 2013. A non-collisional, accretionary Sveconorwegian orogen. Terra Nova 25, 30–37. https://doi.org/10.1111/ter.12001.

Slagstad, T., Roberts, N.M.W., Kulakov, E., 2017. Linking orogenesis across a supercontinent; the Grenvillian and Sveconorwegian margins on Rodinia. Gondwana Res. 44, 109–115.

Slagstad, T., Roberts, N.M.W., Coint, N., Høy, I., Sauer, S., Kirkland, C.L., Marker, M., Røhr, T.S., Henderson, I.H.C., Stormoen, M.A., Skår, Ø., Sørensen, B.E., Bybee, G., 2018. Magma-driven, high-grade metamorphism in the Sveconorwegian Province, southwest Norway, during the terminal stages of Fennoscandian Shield evolution. Geosphere 14, 861–882. https://doi.org/10.1130/GES1565.1.

Slagstad, T., Kulakov, E., Kirkland, C.L., Roberts, N.M.W., Ganerød, M., 2019. Breaking the Grenville-Sveconorwegian link in Rodinia reconstructions. Terra Nova. https://doi.org/10.1111/ter.12406.

Slama, J., Pedersen, R.-B., 2015. Zircon provenance of SW Caledonian phyllites reveals a distant Timanian sediment source. J. Geol. Soc., London 172, 465–478.

Slama, J., 2016. Rare late Neoproterozoic detritus in SW Scandinavia as a response to distant tectonic processes. Terra Nova 28, 394–440.

Stacey, J.S., Kramers, J.D., 1975. Approximation of terrestrial lead isotope evolution by a

two-stage model. Earth Planet. Sci. Lett. 34, 207–226.

Strachan, R.A., Holdsworth, R.E., Krabbendam, M., Alsop, G.I., 2010. The Moine Supergroup of NW Scotland: insights into the analysis of polyorogenic supracrustal sequences. In: Law, R.D., Butler, R.W.H., Holdsworth, R.E., Krabbendam, M., Strachan, R.A. (Eds.), Continental Tectonics and Mountain Building: The Legacy of Peach and Horne. Geological Society, London, pp. 233–254 doi: 10.1144/SP335.11, Special Publications 335.

Tilston, N.C., 1983. Structural Geology and Petrology of the Sygnefjell Area, Northwest Jotunheim, Norway.   PhD thesis. Bedford College (University of London), pp. 411.

Vander Auwera, J., Bogaerts, M., Liégeois, J.-P., Demaiffe, D., Wilmart, E., Bolle, O.,

Duchesne, J.-C., 2003. Derivation of the 1.0-0.9 Ga ferro-potassic A-type granitoids of southern Norway by extreme differentiation from basic magmas. Precambr. Res. 124, 107–148.

Vernikovsky, V.A., Metelkin, D.V., Vernikovskaya, A.E., Sal'nikova, E.B., Kovach, V.P., Kotov, A.B., 2011. The Oldest Island Arc Complex of Taimyr: Concerning the Issue of the Central-Taimyr Accretionary Belt Formation and Paleogeodynamic Reconstructions in the Arctic. Doklady Earth Sci. 436, 186–192.

Watt, G.R., Thrane, K., 2001. Early Neoproterozoic events in East Greenland. Precambr. Res. 110, 164–184.